Universal Transitions between Growth and Dormancy via Intermediate Complex Formation

Jumpei F. Yamagishi[1] and Kunihiko Kaneko[2,3]
[1]Department of Basic Science, The University of Tokyo, 3-8-1 Komaba, Meguro-ku, Tokyo 153-8902, Japan
[2]Center for Complex Systems Biology, Universal Biology Institute, University of Tokyo, 3-8-1 Komaba, Meguro-ku, Tokyo 153-0041, Japan
[3]Niels Bohr Institute, University of Copenhagen, Blegdamsvej 17, 2100 Copenhagen, Denmark

(Received 14 April 2023; accepted 30 January 2024; published 12 March 2024)

A simple cell model consisting of a catalytic reaction network with intermediate complex formation is numerically studied. As nutrients are depleted, the transition from the exponential growth phase to the growth-arrested dormant phase occurs along with hysteresis and a lag time for growth recovery. This transition is caused by the accumulation of intermediate complexes, leading to the jamming of reactions and the diversification of components. These properties are generic in random reaction networks, as supported by dynamical systems analyses of corresponding mean-field models.

DOI: 10.1103/PhysRevLett.132.118401

As microbial cells proliferate, they are crowded and nutrients in the environment are depleted. The cells then enter the dormant phase (or the so-called stationary phase), in which cell growth is significantly arrested [1]. This behavior is commonly observed across microbial species and even mammalian cells under a variety of environmental conditions [2]. In fact, most microbial cells in natural ecosystems are in the growth-arrested dormant phase, as they are under resource limitation [3–7]. Once cells enter the dormant phase, the intracellular metabolic phenotypes drastically change, whereas bistability and hysteresis between the states with exponential and arrested growth are observed as a bimodal distribution of cell growth [8] and are suggested theoretically [9]. Once the cell is in the dormant phase, a certain time is required to recover growth even after the resource supply has resumed; this is known as the lag time [10–12].

Despite the importance of such universal and mundane behavior, the theoretical understanding of dormancy is still in its infancy compared to that of the exponential growth phase, for which well-established quantitative theories are available [13–15]. Although specific molecular mechanisms of dormancy have been extensively studied [4,16], little attention has been paid to establishing a theory for universal characteristics of the dormant phase and transitions to it. References [17,18] represent a few early exceptions. In Ref. [17], by assuming that nutrient limitation leads to the accumulation of waste chemicals, a phenomenological model for the growth-dormant transition was proposed and quantitative laws of the lag time were derived. In Ref. [18], an abstract spin glass model for aging dynamics was proposed. However, the mechanism of the growth-dormant transition and the origin of its universality across species have not been fully explored. Therefore, a better understanding of the growth-dormant transition as a universal behavior of cells growing through intracellular reactions with many components is required.

In this Letter, by considering a simple cell model consisting of catalytic reactions of many components, we demonstrate that such a transition between growth and dormant phases generally appears without specifically tuning the intracellular reactions, as long as intermediate complexes between substrates and catalysts have sufficient lifetimes. The transition is caused by the accumulation of complexes under the depletion of nutrients, and it is characterized as a cusp bifurcation in dynamical systems theory. The transition observed in random reaction networks is then analyzed using "mean-field" models of catalytic reaction dynamics, which also implies that the transition to a dormant phase does not require any special mechanism and is a universal feature of cells that grow by intracellular catalytic reactions.

Model.—In this Letter, we adopt a simple model of cellular dynamics that captures only the basic features of these dynamics. It consists of intracellular reaction networks and transport reactions of externally supplied nutrient(s). Complicated intracellular metabolic reactions are simplified as randomly connected catalytic reaction networks. Although such models with catalytic reaction networks have reproduced the statistics of cells in the exponential growth phase [19,20], they do not demonstrate

the growth-dormant transition. One possible drawback of these models is that catalytic reactions progress immediately. In reality, each chemical reaction progresses after the formation of an intermediate complex between the substrate and the catalyst is formed.

We introduce a model that includes the formation of intermediate complexes in reactions and examine whether and how the growth-dormant transition is exhibited by the model. Then, each catalytic reaction ρ, in which substrate X_{ρ_s} is converted into product X_{ρ_p} by catalyst X_{ρ_c}, consists of two-step elementary reaction processes with the formation of an intermediate complex Y_ρ as follows:

$$X_{\rho_s} + X_{\rho_c} \underset{k_\rho^-}{\overset{k_\rho^+}{\rightleftharpoons}} Y_\rho \xrightarrow{v_\rho} X_{\rho_p} + X_{\rho_c}.$$

Here, each elementary process proceeds according to the law of mass action with the labeled coefficient, and ρ_s, ρ_p, and ρ_c denote the indices of the substrate, product, and catalyst for reaction ρ, respectively. For the adiabatic limit $v_\rho \to \infty$, the above reaction processes are reduced to the single mass action kinetics without intermediate complex formation, $X_{\rho_s} + X_{\rho_c} \to X_{\rho_p} + X_{\rho_c}$, and the model is reduced to those studied earlier [19,20]. In contrast, when v_ρ is small, the intermediate complex Y_ρ can accumulate, leading to a decrease in free reactants that are not bound to complexes, which can hinder the reaction processes.

Considering a cell consisting of n chemicals and N_r reactions (and the corresponding intermediate complexes), its state is represented by a set of concentrations $(\mathbf{x}, \mathbf{y})$ of free reactants X_i and complexes Y_ρ. The time change of the cellular state $(\mathbf{x}, \mathbf{y})$ is then given as follows:

$$\dot{x}_i = \sum_\rho [(\delta_{i,\rho_p} + \delta_{i,\rho_c}) v_\rho y_\rho - (\delta_{i,\rho_s} + \delta_{i,\rho_c}) f_\rho(\mathbf{x}, \mathbf{y})] + F_i(\mathbf{x}; S_{\mathrm{ext}}, \alpha) - \mu x_i, \tag{1}$$

$$\dot{y}_\rho = f_\rho(\mathbf{x}, \mathbf{y}) - v_\rho y_\rho - \mu y_\rho, \tag{2}$$

where $f_\rho(\mathbf{x}, \mathbf{y}) \coloneqq k_\rho^+ x_{\rho_s} x_{\rho_c} - k_\rho^- y_\rho$ is the total consumption rate of substrate ρ_s by reaction ρ, and δ is Kronecker's delta. The term $F_i(\mathbf{x}; S_{\mathrm{ext}}, \alpha)$ in Eq. (1) represents the intake of chemical X_i ($i = 0, 1, \ldots, n-1$), which can be nonzero if X_i is a nutrient but is zero otherwise. The last terms in Eqs. (1) and (2), $-\mu x_i$ and $-\mu y_\rho$, represent the dilution of each concentration due to cellular volume growth. The growth rate μ is given by $\mu(\mathbf{x}, \mathbf{y}) \coloneqq \sum_i F_i(\mathbf{x})$, because for simplicity we assumed that the contribution of each chemical X_i to volume or weight is uniform regardless of i. $\sum_i x_i + 2\sum_\rho y_\rho = 1$ is then constant in the dynamics (1) and (2) based on the law of mass conservation.

Below, for simplification purposes, the reaction rate constants k_ρ^+, k_ρ^-, and v_ρ are set as independent of ρ, and they are denoted by $k^+ = 1$, $k^- = 0$, and v, respectively [21]. For simplicity, we also assumed that there is only a single nutrient chemical X_0. Its intake is mediated by transporter chemical X_1 with $\alpha = 2$, i.e., $F_i(\mathbf{x}; S_{\mathrm{ext}}, \alpha) = \delta_{i0} S_{\mathrm{ext}} x_1^\alpha$, where S_{ext} denotes the environmental concentration of nutrient chemical X_0, and the transport coefficient for F_i is normalized as unity. Note that the following results and arguments hold independent of the details of settings, such as parameter values and specific functional forms of nutrient intake F_i [see also Sec. A of the Supplemental Material (SM) [22]].

Randomly generated networks.—To understand the behaviors of the above model, we first randomly generated hundreds of intracellular reaction networks [26]. The steady state $\mathbf{x}^*$ for each reaction network was numerically calculated. We here numerically confirmed that there is a unique steady state for each of the growth and dormant phases [27]. We then observed discontinuous transitions between growth and dormant phases against external nutrient abundance S_{ext}.

As an example, we consider the reaction network in Fig. 1(a). In Fig. 1(b), the steady growth rate μ^*, numerically obtained by solving the dynamics (1) and (2), is plotted against the environmental nutrient concentration S_{ext}. As shown, μ^* drops by orders of magnitude at a certain value of S_{ext}, denoted by S_{ext}^c, thus demonstrating the transition from growth to the growth-arrested dormant phase. In addition, when S_{ext} is increased starting with the dormant phase, the transition occurs at a larger S_{ext}, thus demonstrating hysteresis and bistability between the growth and dormant phases with intermediate levels of nutrient supply S_{ext} [Fig. 1(b)] [28], as is observed for real microbes [8].

Through this *growth-dormant transition*, the intracellular chemical compositions and dominant reactions at work also change drastically [Figs. 1(b) and 1(c)]. In the growth phase with larger S_{ext}, the nutrient influx is concentrated on an *autocatalytic growth subnetwork* (AGS) [30–34] consisting of a few chemicals and reactions that connect the nutrient to the transporter (and its associated by-products). In contrast, in the dormant phase, fluxes spread over many chemicals in subnetworks that cannot sustain growth by themselves and are parasitic on the AGS; i.e., the synthesis of their components is supported by the AGS but does not support the synthesis of the AGS. We call these the *nongrowing subnetwork* (NGS) (see Sec. A of the SM [22] for details). These subnetworks compete with each other while also overlapping: activation of the AGS suppresses the NGS via growth-induced dilution, while the latter inhibits the former when the NGS can replicate autocatalytically by consuming some chemical in the AGS; moreover, reactants bound as a complex in the NGS cannot work for reactions in the AGS, and vice versa. Consistently, the total concentration of complexes $Y \coloneqq \sum_\rho y_\rho^*$ and the complexes within the NGS increase across the growth-dormant transition, as shown in Fig. 1(d). Owing to the

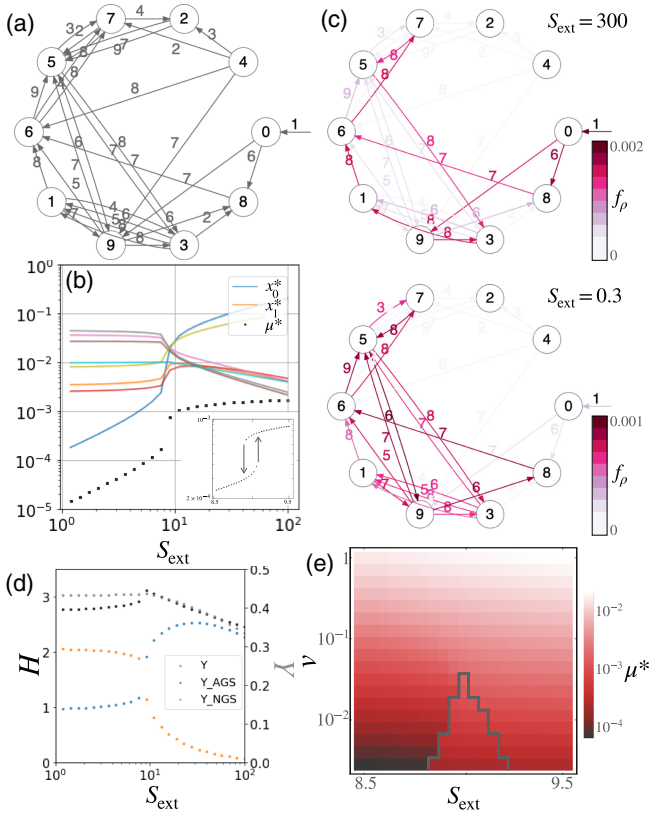

FIG. 1. Example of a growth-dormant transition in randomly generated networks. (a) Reaction network ($n = 10$, $N_r = 30$). Chemicals at arrow tails are transformed into those at arrow heads, catalyzed by the chemicals labeled on the edges. Nutrient X_0 is taken up via active transport by transporter X_1 in proportion to x_1^2. (b) Dependence of μ^* (black points) and x_i^* (colored lines) on S_{ext}. $v = 0.01$. $S_{ext}^c \simeq 8.9$. Each different color denotes a different i. Inset: Hysteresis and bistability for μ^*. (c) Dominant pathways for the growth phase ($S_{ext} = 300$; top sketch) and dormant phase ($S_{ext} = 0.3$; bottom sketch). $v = 0.01$. The edge colors represent reaction fluxes in the log scale. (d) Dependence of composition entropy $H := -\sum_i x_i^* \log x_i^* - \sum_\rho 2y_\rho^* \log(2y_\rho^*)$ (black line) as well as $Y := \sum_\rho y_\rho^*$ (gray line) and total concentrations of complexes in the AGS ($Y_{AGS} := \sum_{\rho \in AGS} y_\rho^*$; blue line) and in the NGS ($Y_{NGS} := \sum_{\rho \in NGS \setminus AGS} y_\rho^*$; orange line) on S_{ext}. $v = 0.01$. (e) Dependence of μ^* on (S_{ext}, v). μ^* is numerically calculated by decreasing S_{ext} for each v, and hysteresis is numerically observed in the area surrounded by the gray line.

competition between the AGS and the NGS, this transition exhibits discontinuity, hysteresis, and bistability [Figs. 1(b) and 1(e)]. Indeed, without such a NGS being parasitic on the AGS, the growth-dormant transition does not occur (Fig. S2 of the SM [22]).

To measure such competition, we defined the *composition entropy* $H(\mathbf{x}, \mathbf{y}) := -\sum_i x_i \log x_i - \sum_\rho 2y_\rho \log(2y_\rho)$, which quantifies the diversity of cellular components. In general, in the growth phase, the AGS with the largest growth rate should be dominant and H is small, whereas in the dormant phase, many reactions and chemicals in the

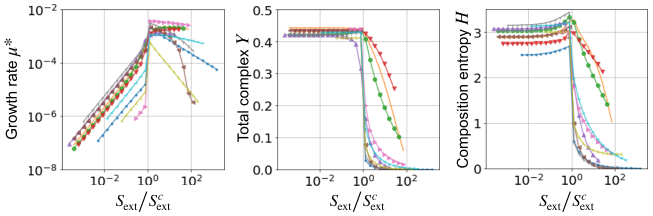

FIG. 2. Steady growth rate μ^*, total concentration of complexes Y, and composition entropy H plotted against S_{ext}/S_{ext}^c for randomly generated networks exhibiting growth-dormant transitions in different colors. $n = 10, N_r = 30$, and $v = 0.01$.

NGS are involved to a similar extent, and thus H can be relatively large. As both subnetworks are comparably active near the critical nutrient concentration S_{ext}^c, the composition entropy H, or the diversity of the intracellular chemical composition reaches a maximum near the transition point [Fig. 1(d)]. Notably, such a trend is common among randomly generated networks (Fig. 2) [35]. From a biological perspective, this prediction would be consistent with the observations that stringent responses increase the diversity of the cellular components during the transition and in the dormant phase [4,16,36].

The suppression of growth at the transition can be understood as a type of jamming caused by the accumulation of intermediate complexes [37]: the occupation of complexes in the NGS limits the free catalysts necessary for reactions in the AGS since it causes further occupation of complexes in the NGS, leading to a cascading effect similar to the jamming process. Consistently, if v is sufficiently large, discontinuous transition and hysteresis are not observed against changes in S_{ext} [Fig. 1(e)]. Moreover, the dependence of the steady growth rate μ^* on (S_{ext}, v) in Fig. 1(e) suggests a cusp bifurcation in the dynamical systems theory (as is also confirmed by the following mean-field analysis) [38]. We also found that as v is smaller, both S_{ext}^c and μ_{max} are smaller; in other words, when v varies, a trade-off occurs between maximum growth rate μ_{max} and minimal nutrient concentration for the growth phase, S_{ext}^c. Such a trade-off has historically been considered a result of evolution leading to adaptations to either abundant or scarce nutrient environments [42,43], whereas our results suggest that this trade-off is a universal feature of growing cells with complex reaction networks.

Statistically, sufficiently large reaction networks are expected to include NGSs in addition to AGSs. Indeed, even with $n = 10$–30, about half of the randomly generated networks exhibited growth-dormant transitions [Fig. S3(a) of the SM [22]]. In addition, the proportion of networks that exhibit transitions is maximal for relatively sparse reaction networks, and the peak value gradually increases as the number n of chemicals increases. The following characteristics are also common to such networks: (i) growth-dormant transition against changes in S_{ext} requires small v, i.e., sufficient residence time for the complexes; (ii) hysteresis

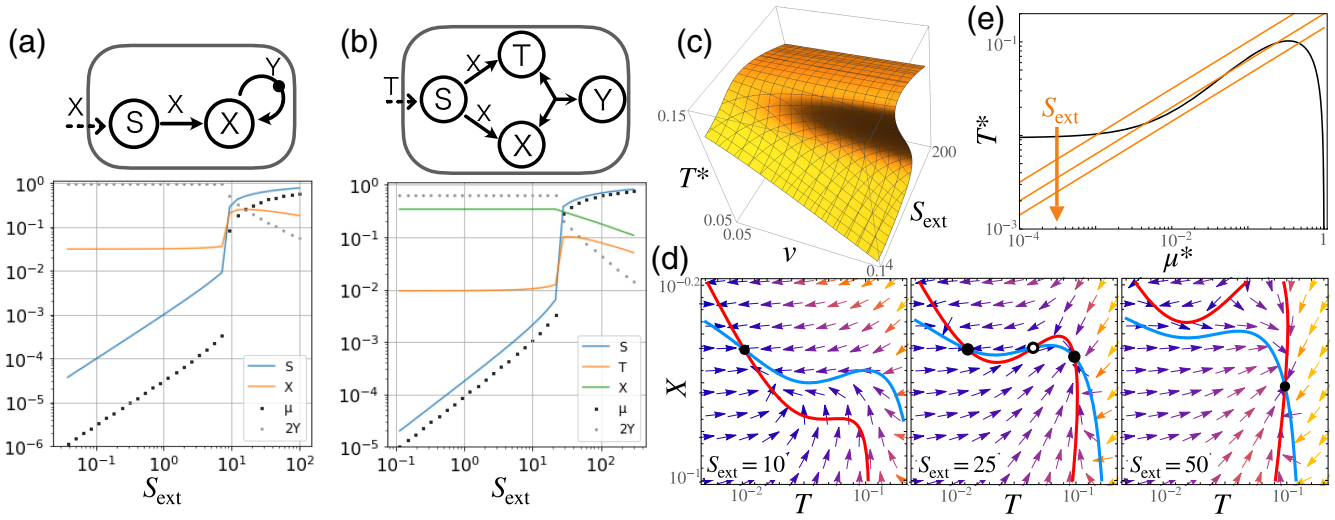

FIG. 3. Mean-field models. (a) Mean-field model with S, X, and Y only. Top sketch: network structure. Bottom panel: dependence of μ^* and steady states on S_{ext}. $S_{ext}^c \simeq 9.3$, $\alpha = 3$, and $v = 0.001$. (b)–(e) Mean-field model with the distinction between transporter T and the remaining chemicals X. Unless otherwise stated, $v = 0.01$ and $n_X = 2$. (b) Top sketch: network structure. Bottom panel: dependence of μ^* and steady states on S_{ext}. $S_{ext}^c \simeq 21.9$. (c) Bifurcation diagram: Dependence of T^* on (S_{ext}, v) in the log scale. (d) Flow diagram in the phase space (T, X). The red and blue lines represent T nullcline and X nullcline, respectively. Arrows with brighter colors correspond to faster flows. (e) Self-consistent equation for T and μ. The black and orange lines depict $T = T^*(\mu; v, n_X)$ [Eq. (B1) of the SM [22]] and $T = (\mu/S_{ext})^{1/\alpha}$ with $S_{ext} = 10$, 25, 50, respectively.

against changes in S_{ext}; (iii) increases in composition entropy H around the transitions; and (iv) a trade-off between maximum growth rates μ_{max} and minimal nutrient concentrations S_{ext}^c to sustain growth. These results, presented theoretically for the first time and in agreement with experiments, suggest the universality of growth-dormant transitions due to reactant competition via complex formation in complicated reaction networks, as is the case for metabolic networks in real microbes.

Lag time.—We also numerically calculated the time for growth recovery after starvation as follows: First, up to $t = 0$, cells are set in nutrient-rich conditions with sufficiently large S_{ext}, remaining in steady states with exponential growth. At $t = 0$, the external nutrient supply is instantaneously depleted to $S_{ext} = 0$ until $t = T_{stv}$. Finally, S_{ext} is instantaneously increased to the original value. Then, a certain period $T_{lag} \gg 1/\mu_{max}$, known as the lag time, is required for the cell to recover the original exponential growth if the NGS is not a cycle and the amount of transporter chemical is sufficiently reduced therein; here, the lag time T_{lag} increases with starvation time T_{stv} in the form $T_{lag} \propto T_{stv}^{\beta}$ for a certain range (up to some saturation time) (see Fig. S4 of the SM [22] for an example and Sec. A for more details). Here, the concentration of the transporter gradually decreased during starvation, and the growth recovery requires the regain of the transporter and the alleviation of the jamming that occurred during the dormant phase; as a result, the lag time increases with the starvation time. The exponent β ranges approximately from 0.3 to 0.5, depending on the network structures that alter the intracellular reaction dynamics. This result is consistent with the experimental measurements [44,45] (Fig. S5 of the SM [22]).

Mean-field analysis.—To further investigate the mechanism underlying the growth-dormant transition in terms of dynamical systems theory, we constructed mean-field models. First, we considered a model with one effective concentration variable X and the associated complexes Y in addition to the nutrient S [Fig. 3(a)]. It exhibits the growth-dormant transition, whereas this model with minimal structure requires the nonlinearity in transport $\alpha > 2$ and extremely small $v < \mu_{max}$.

Then, we considered another mean-field model that incorporates another variable T representing the mean field for the concentration of the transporter(s) in addition to X representing the remaining non-nutrient chemicals [Fig. 3(b)]. The number of chemicals represented by X and T are denoted by n_X and n_T, respectively. As only the complex Y between X and T is considered for simplicity in this model [46], it includes the AGS, $S + X \to T + X$ and $S + X \to 2X$, and the single NGS, $T + X \rightleftharpoons Y$. This mean-field model reproduces common behaviors observed for randomly generated networks, including discontinuous growth-dormant transitions with $v > \mu_{max}$ [Fig. 3(b)]. The transition occurs when $n_X > n_T = 1$, and a larger number n_X of X leads to a larger S_{ext}^c (Fig. S9 of the SM [22]).

From the bifurcation analysis [Figs. 3(c) and 3(d)], we found that the growth-dormant transition occurs as a cusp bifurcation against changes in S_{ext} and v [47]. This observation can explain discontinuous transitions and hysteresis. Notably, although both the transporter T and

the remaining chemicals X are essential for cell growth, their competition leads to a flow field with mutual inhibition as in the toggle switch at the intermediate value of S_{ext}. Furthermore, from the self-consistent equation for the steady growth rate μ^*, we can determine where and how the growth-dormant transition occurs [Fig. 3(e)].

Discussion.—In this Letter, we studied a model of catalytic reaction networks wherein a variety of components react via the formation of intermediate complexes. This model exhibits discontinuous growth-dormant transitions against nutrient conditions as long as the formed complexes have sufficient lifetimes (i.e., they have small v). This transition to growth-arrested dormant phases is caused by the accumulation of intermediate complexes in the NGS under nutrient-poor conditions, which results in the jamming of reactions in the AGS. Remarkably, other basic characteristics of dormancy, i.e., hysteresis between the exponential growth and dormant phases, the lag time for growth recovery after starvation, and a trade-off between the maximum growth rate μ_{max} and the minimal nutrient concentration S^c_{ext} to sustain growth (in other words, a sort of sensitivity to nutrient scarcity) are also reproduced. The above mechanism is general; any cellular metabolic system allowing exponential growth must contain an AGS, and the presence of a NGS could also be generic for complicated reaction networks. Although we mainly investigated randomly generated networks and mean-field models reduced from them to reveal a general mechanism, a metabolic reaction network simplified from real data [48] can also show the growth-dormant transition (see Fig. S7 of the SM [22]). Further studies of detailed, realistic models, such as those including distributed parameters and more realistic network structures, will be necessary to reveal how the above fundamental characteristics of dormancy are preserved or changed by evolution.

These results indicate that growth-dormant transitions and dormancy might be inevitable for cells that grow via complex-forming catalytic reaction networks and likely emerge without tuning by evolution or adaptation; thus, even protocells at the primitive stage of life [49,50] are expected to exhibit such transitions to dormancy, which would be relevant to their survival under environmental stress. In this Letter, the existence of intermediate complexes is essential, while they can be any molecules. Candidates for specific molecules include the complex of ribosome and the ribosome-binding factors such as the hibernation promoting factors [51] as well as the intermediate metabolites of the citric acid cycle and the pentose phosphate pathway [52].

The composition entropy H is predicted to increase toward the transition point as a result of the competition between the AGS and the NGS, which is experimentally verifiable. From a biological perspective, the stringent responses would increase the diversity of the intracellular components [4,16,36].

We also analyzed the dynamics of mean-field models and thereby demonstrated that the growth-dormant transition occurs as a cusp bifurcation, which supports the discontinuity of the transitions as well as hysteresis. The validity of the coarse-grained mean-field models implies that the occurrence and mechanism of the growth-dormant transition do not depend on details of the reaction networks; e.g., it suggests the universality of the growth-dormant transition across many-body reaction systems [53].

Finally, while this Letter examined the growth-dormant transition primarily at the single-cell level, the behaviors observed in practice often manifest at the population level, which may be an intriguing avenue for future research. By adopting stochastic simulations, the cell-to-cell variation within a population can be computed, which will lead to the emergence of a bimodal distribution in the hysteresis regime [8,55].

In conclusion, our Letter explained the ubiquity and fundamental characteristics of dormancy as general properties in reaction networks with complex formation by offering a coherent view of cell growth and dormancy.

The authors would like to thank Yuichi Wakamoto, Yusuke Himeoka, Tetsuhiro S. Hatakeyama, and Shuji Ishihara for the stimulating discussions. J. F. Y. is supported by a grant-in-aid for JSPS Fellows (Grant No. 21J22920) and the Masason Foundation. K. K. is supported by Grant-in-Aid for Scientific Research (A) No. 20H00123 from the Ministry of Education, Culture, Sports, Science, and Technology (MEXT) of Japan and Novo Nordisk Foundation Grant No. NNF21OC0065542.

[1] Such growth-arrested states are often referred to as dormant, nongrowing, or quiescent state, as well as stationary phase for cellular populations. Herein, we adopt the term *dormant phase*.

[2] J. V. Gray, G. A. Petsko, G. C. Johnston, D. Ringe, R. A. Singer, and M. Werner-Washburne, "Sleeping beauty": Quiescence in Saccharomyces cerevisiae, Microbiol. Mol. Biol. Rev. **68**, 187 (2004).

[3] S. E. Finkel, Long-term survival during stationary phase: Evolution and the GASP phenotype, Nat. Rev. Microbiol. **4**, 113 (2006).

[4] J. M. Navarro Llorens, A. Tormo, and E. Martínez-García, Stationary phase in gram-negative bacteria, FEMS Microbiol. Rev. **34**, 476 (2010).

[5] P. A. Del Giorgio and J. M. Gasol, Physiological structure and single-cell activity in marine bacterioplankton, Microbial Ecol. Oceans **2**, 243 (2008).

[6] O. Gefen, O. Fridman, I. Ronin, and N. Q. Balaban, Direct observation of single stationary-phase bacteria reveals a surprisingly long period of constant protein production activity, Proc. Natl. Acad. Sci. U.S.A. **111**, 556 (2014).

[7] D. L. Kirchman, *Processes in Microbial Ecology* (Oxford University Press, New York, 2018), Chap. 6.

[8] O. Kotte, B. Volkmer, J. L. Radzikowski, and M. Heinemann, Phenotypic bistability in Escherichia coli's central carbon metabolism, Mol. Syst. Biol. **10**, 736 (2014).
[9] S. Krishna and S. Laxman, A minimal "push-pull" bistability model explains oscillations between quiescent and proliferative cell states, Mol. Biol. Cell **29**, 2243 (2018).
[10] I. Levin-Reisman, O. Gefen, O. Fridman, I. Ronin, D. Shwa, H. Sheftel, and N. Q. Balaban, Automated imaging with scanlag reveals previously undetectable bacterial growth phenotypes, Nat. Methods **7**, 737 (2010).
[11] A. Jõers and T. Tenson, Growth resumption from stationary phase reveals memory in Escherichia coli cultures, Sci. Rep. **6**, 24055 (2016).
[12] Y. Kaplan, S. Reich, E. Oster, S. Maoz, I. Levin-Reisman, I. Ronin, O. Gefen, O. Agam, and N. Q. Balaban, Observation of universal ageing dynamics in antibiotic persistence, Nature (London) **600**, 290 (2021).
[13] M. Scott and T. Hwa, Bacterial growth laws and their applications, Curr. Opin. Biotechnol. **22**, 559 (2011).
[14] K. Kaneko, C. Furusawa, and T. Yomo, Universal relationship in gene-expression changes for cells in steady-growth state, Phys. Rev. X **5**, 011014 (2015).
[15] S. Jun, F. Si, R. Pugatch, and M. Scott, Fundamental principles in bacterial physiology—History, recent progress, and the future with focus on cell size control: A review, Rep. Prog. Phys. **81**, 056601 (2018).
[16] J. Jaishankar and P. Srivastava, Molecular basis of stationary phase survival and applications, Front. Microbiol. **8**, 2000 (2017).
[17] Y. Himeoka and K. Kaneko, Theory for transitions between exponential and stationary phases: Universal laws for lag time, Phys. Rev. X **7**, 021049 (2017).
[18] S. Reich, S. Maoz, Y. Kaplan, H. Rappeport, N. Balaban, and O. Agam, Slow relaxation and aging in the model of randomly connected cycles network, Phys. Rev. Res. **4**, 033127 (2022).
[19] C. Furusawa and K. Kaneko, Zipf's law in gene expression, Phys. Rev. Lett. **90**, 088102 (2003).
[20] C. Furusawa and K. Kaneko, Adaptation to optimal cell growth through self-organized criticality, Phys. Rev. Lett. **108**, 208103 (2012).
[21] Note that the model's behavior does not depend on k^- (see also Fig. S1 of the SM [22]).
[22] See Supplemental Material at http://link.aps.org/supplemental/10.1103/PhysRevLett.132.118401, which includes Refs. [23–25], for more details on the AGS and NGS, the lag time, and the mean-field analysis, as well as additional data on our model.
[23] D. H. de Groot, J. Hulshof, B. Teusink, F. J. Bruggeman, and R. Planqué, Elementary growth modes provide a molecular description of cellular self-fabrication, PLoS Comput. Biol. **16**, e1007559 (2020).
[24] S. Müller, Elementary growth modes/vectors and minimal autocatalytic sets for kinetic/constraint-based models of cellular growth, bioRxiv (2021).
[25] C. H. Schilling, D. Letscher, and B. Ø. Palsson, Theory for the systemic definition of metabolic pathways and their use in interpreting metabolic function from a pathway-oriented perspective, J. Theor. Biol. **203**, 229 (2000).
[26] The reaction networks are generated by randomly selecting the combination of substrates, catalysts, and products for N_r reactions. Substrates and catalysts are chosen so that no reactions are autocatalytic. Also, the nutrient chemical X_0 can only be a substrate of intracellular reactions, and transporter chemical X_1 cannot catalyze any intracellular reactions.
[27] Oscillation can occur with some networks, but such networks are rare. The oscillation is due to a positive feedback of the transporter abundance to the nutrient abundance with delay and does not occur near the growth-dormant transition.
[28] In this Letter, unless otherwise noted, we plot the steady states that cells reach when $S_{\rm ext}$ is lowered; i.e., the initial state for each set of parameters is given as the steady state with slightly higher $S_{\rm ext}$. In real cells, the fluctuation of internal concentrations leads to attractor selection [29]; thus, the branch with the higher growth rate would be more likely to be observed.
[29] A. Kashiwagi, I. Urabe, K. Kaneko, and T. Yomo, Adaptive response of a gene network to environmental changes by fitness-induced attractor selection, PLoS One **1**, e49 (2006).
[30] M. Eigen and P. Schuster, *The Hypercycle: A Principle of Natural Self-Organization* (Springer Science+Business Media, New York, 2012).
[31] S. A. Kauffman *et al.*, *The Origins of Order: Self-Organization and Selection in Evolution* (Oxford University Press, New York, 1993).
[32] S. Jain and S. Krishna, Autocatalytic sets and the growth of complexity in an evolutionary model, Phys. Rev. Lett. **81**, 5684 (1998).
[33] K. Kaneko, On recursive production and evolvability of cells: Catalytic reaction network approach, Adv. Chem. Phys. **130**, 543 (2005).
[34] A. Blokhuis, D. Lacoste, and P. Nghe, Universal motifs and the diversity of autocatalytic systems, Proc. Natl. Acad. Sci. U.S.A. **117**, 25230 (2020).
[35] The $S_{\rm ext}$ dependence differs between networks due to a limited number of chemical components, i.e., the small size of the networks. With some networks, μ decreases as $S_{\rm ext}$ increases in the growth phase, while the other characteristics for the growth-dormant transition presented here are conserved (Fig. S1 of the SM [22]).
[36] R. Nirupama, B. Rajaraman, and H. Yajurvedi, Stress and glucose metabolism: A review, Imag. J. Clin. Med. Sci. **5**, 8 (2018).
[37] T. S. Hatakeyama and C. Furusawa, Metabolic dynamics restricted by conserved carriers: Jamming and feedback, PLoS Comput. Biol. **13**, e1005847 (2017).
[38] Similarly, the jamming transition in the traffic of self-driven particles can be understood as a saddle-node bifurcation in terms of the dynamical-systems theory [39]. Notably, hysteresis, as observed in this Letter, is also a characteristic of conventional jamming phenomena [40,41].
[39] M. Fujii, A. Awazu, and H. Nishimori, Saddle-node bifurcation to jammed state for quasi-one-dimensional counter-chemotactic flow, Phys. Rev. E **82**, 015102(R) (2010).
[40] O. Braun, B. Hu, A. Filippov, and A. Zeltser, Traffic jams and hysteresis in driven one-dimensional systems, Phys. Rev. E **58**, 1311 (1998).

[41] D. Head, A. Ajdari, and M. Cates, Jamming, hysteresis, and oscillation in scalar models for shear thickening, Phys. Rev. E **64**, 061509 (2001).
[42] B. Shipley and P. Keddy, The relationship between relative growth rate and sensitivity to nutrient stress in twenty-eight species of emergent macrophytes, J. Ecol. **76**, 1101 (1988).
[43] J. W. Fink, N. A. Held, and M. Manhart, Microbial population dynamics decouple growth response from environmental nutrient concentration, Proc. Natl. Acad. Sci. U.S.A. **120**, e2207295120 (2023).
[44] C. Pin and J. Baranyi, Single-cell and population lag times as a function of cell age, Appl. Environ. Microbiol. **74**, 2534 (2008).
[45] J.-C. Augustin, L. Rosso, and V. Carlier, A model describing the effect of temperature history on lag time for Listeria monocytogenes, International Journal of food microbiology **57**, 169 (2000).
[46] There are several possibilities for the choice of mean-field models with effective reactions among X and T that exhibit the growth-dormant transition (see Sec. B of the SM [22]).
[47] V. I. Arnold, *Geometrical Methods in the Theory of Ordinary Differential Equations*, Grundlehren der Mathematischen Wissenschaften Vol. 250 (Springer Science+Business Media, New York, 1988).
[48] G. Bastin, Quantitative analysis of metabolic networks and design of minimal bioreaction models, *Revue Africaine de Recherche en Informatique et Mathématiques Appliquées*, Vol. 9 (2008), 10.46298/arima.1891.
[49] P. L. Luisi, *The Emergence of Life: From Chemical Origins to Synthetic Biology* (Cambridge University Press, Cambridge, England, 2016).
[50] S. Ameta, Y. J. Matsubara, N. Chakraborty, S. Krishna, and S. Thutupalli, Self-reproduction and Darwinian evolution in autocatalytic chemical reaction systems, Life **11**, 308 (2021).
[51] M. Ueta, R. L. Ohniwa, H. Yoshida, Y. Maki, C. Wada, and A. Wada, Role of HPF (hibernation promoting factor) in translational activity in Escherichia coli, J. Biochem. **143**, 425 (2008).
[52] Z. Rashida and S. Laxman, The pentose phosphate pathway and organization of metabolic networks enabling growth programs, Curr. Opin. Syst. Biol. **28**, 100390 (2021).
[53] Although the mean-field models in Fig. 3 capture the mechanism of the dormancy or growth arrest due to complex accumulation, the diversification of components in nutrient-poor conditions owing to competition between subnetworks [54] is not addressed. To consider such diversification and improve the mean-field theory, the incorporation of two-body correlations among the concentrations beyond their mean will be required.
[54] A. Kamimura and K. Kaneko, Negative scaling relationship between molecular diversity and resource abundances, Phys. Rev. E **93**, 062419 (2016).
[55] In this case, at the population level, the dependence of growth rate on nutrient level may be more gradual due to mixing effects, and transient growth rates may show a more gradual response.